Available online at www.sciencedirect.com

SciVerse ScienceDirect

Ceramics International 39 (2013) 2795–2802

CERAMICS INTERNATIONAL

www.elsevier.com/locate/ceramint

Butyl rubber–$Ba_{0.7}Sr_{0.3}TiO_3$ composites for flexible microwave electronic applications

Janardhanan Chameswary, Mailadil Thomas Sebastian*

Materials Science and Technology Division, National Institute for Interdisciplinary Science and Technology (CSIR), Trivandrum 695019, India

Received 20 July 2012; received in revised form 13 September 2012; accepted 13 September 2012
Available online 7 October 2012

Abstract

Butyl rubber–$Ba_{0.7}Sr_{0.3}TiO_3$ composites (BR–BST) were prepared by sigma mixing followed by hot pressing. The stress–strain studies show the good flexibility of the composite. The dielectric properties of the composites were investigated at both radio and microwave frequencies. The relative permittivity (ε_r) and loss tangent (tan δ) improved with filler loading at both the frequencies. The relative permittivity and loss tangent of the BR–BST composites at a maximum filler loading of 0.39 volume fraction (v_f) are 13.1 and 0.009 respectively at 5 GHz measured by Split Post Dielectric Resonator (SPDR). The effective relative permittivity of the BR–BST composites is compared with theoretical models. The variation of ε_r with temperature was also investigated in the range 22–80 °C at 1 MHz. The microwave dielectric properties of the composites are also studied after repeated bending. The coefficient of thermal expansion (CTE) of the butyl rubber–BST composites decreased with the addition of the BST ceramic.

Keywords: A. Hot pressing; B. composites; C. Dielectric properties; C. Mechanical properties

1. Introduction

Recently electronic industry is in search of light weight, stretchable and deformable substrate materials for microwave electronic applications [1]. Today's customary way of electronic industry is the assembly of electronic components on rigid and/or flexible printed circuit boards [2]. The use of flexible electronics is restricted to flat substrates. In contrast to flexible electronics, stretchable electronics can be used for curved surfaces and movable parts such as the joints of a robot's arm, human medical prostheses etc. [3]. The stretchable electronic circuit will integrate different components onto polymer substrate that may be stretched once or many times depending on the application [4]. The stretchable circuit has the ability to withstand large levels of strain without fracture and also no deterioration in the electronic properties [1]. The soft and rubbery future of electronic industry needs new materials to satisfy their requirements [5]. The requirements for a material to be used for flexible dielectric wave guide [6,7] applications are high relative permittivity, low loss tangent, mechanical flexibility, low coefficient of thermal expansion, high thermal conductivity etc. It is very difficult to get a single material with all the above mentioned properties. There are ceramics with high relative permittivity and low loss tangent. But their brittle nature restricts its use. Low loss polymers are also available. But their high CTE and low thermal conductivity precludes them from practical use. Therefore the application of an individual polymer or ceramic alone is restricted in many aspects. Hence the polymer–ceramic composites can serve better performance than their constituent phases. The conventional polymers such as polyethylene, polystyrene, polypropylene are flexible enough but cannot be used for stretchable applications. The conventional polymers can be replaced by elastomers and the elastomer ceramic composites found applications ranging from ultrathin health monitoring tapes to advanced imaging devices [5].

Many literatures are available on the microwave dielectric properties of polymer–ceramic composites [8–11]. Only a few reports are available in the field of elastomer ceramic composites. Xiang et al. fabricated and investigated the dielectric properties of polyolefin elastomer–$SrTiO_3$ composite with different volume fractions of ceramic filler at the microwave

---

*Corresponding author. Tel.: +91 471 2515294; fax: +91 471 249 1712.
E-mail address: mailadils@yahoo.com (M.T. Sebastian).

0272-8842/$ - see front matter © 2012 Elsevier Ltd and Techna Group S.r.l. All rights reserved.
http://dx.doi.org/10.1016/j.ceramint.2012.09.047

frequency [12]. Janardhanan et al. and Thomas et al. [13,14] reported the microwave dielectric, thermal and mechanical properties of butyl rubber–strontium titanate and butyl rubber–strontium cerium titanate composites respectively. The elastomer chosen for the present study was butyl rubber because of its excellent dielectric properties ($\varepsilon_r \sim 2.44$ and $\tan\delta \sim 10^{-4}$ at 1 MHz), good weathering resistance, flexibility etc. [15]. Barium strontium titante ($Ba_{0.7}Sr_{0.3}TiO_3$) is a well known ferroelectric ceramic with very high relative permittivity ($\varepsilon_r \sim 2850$ at 1 MHz) [16] was chosen as the ceramic filler. Hu et al. investigated the dielectric properties of $Ba_{0.55}Sr_{0.45}TiO_3$–cyclic olefin copolymer composites with different filler loadings with common and nano-size ceramic powders at 1 GHz [17]. Wang et al. prepared $Ba_{0.6}Sr_{0.4}TiO_3$–polymethylmethacrylate composites with 0–3, 1–3 and 2–2 type structures and studied the effect of composite type on the dielectric properties at 10 kHz [18]. Lou et al. studied the dielectric tunability of silicone rubber–$Ba_{0.65}Sr_{0.35}TiO_3$ composites with various volume fractions of ceramic content [19]. Even though dielectric properties of polymer–barium strontium titanate composites are available in the literature, the microwave dielectric properties of butyl rubber–BST composites are not yet reported. The present investigation deals with the synthesis and microwave dielectric, thermal and mechanical characterization of butyl rubber–$Ba_{0.7}Sr_{0.3}TiO_3$ composites.

2. Experimental

$Ba_{0.7}Sr_{0.3}TiO_3$ ceramic was prepared by following the conventional solid state ceramic route. Stoichiometric quantities of $BaCO_3$, $SrCO_3$ and TiO_2 (99.9+%, Sigma-Aldrich) were ball milled for 24 h in distilled water using Yttria-stabilized Zirconia balls in a plastic container. The slurry was dried and calcined at 1100 °C for 6 h. The calcined powder was ground well and sintered at 1300 °C for 4 h. The powder was then sieved through a 25 μm sieve. Butyl rubber–$Ba_{0.7}Sr_{0.3}TiO_3$ composites were prepared by sigma mixing. The compositions for BR–BST-0, BR–BST-1, BR–BST-2, BR–BST-3, BR–BST-4, BR–BST-5, BR–BST-6 and BR–BST-7 are given in Table 1 [20]. The mixing was done in a kneading machine. The composites thus obtained were then hot pressed at 200 °C for 90 min under a pressure of 2 MPa.

The phase purity of the ceramic powder was analyzed by X-ray powder diffraction technique with Cu-Kα radiation (Philips X'Pert PRO MPD X-ray diffractometer). The microstructure of the composites was examined using a Scanning Electron Microscope (SEM) (Jeol Model, JSM 5600LV). Tensile tests on the BR–BST composites were conducted using dumb-bell shaped samples of width ≈4 mm and thickness in the range 1.5–2 mm. The measurements were carried out in a Universal Testing Machine (Hounsfield Model, H5K-S UTM) with a rate of grip separation of 500 mm/min. The dielectric properties at 1 MHz were measured following the parallel plate capacitor method using a LCR meter (Hioki Model, 3532-50). The dielectric properties at 5 GHz were measured by both SPDR and cavity perturbation technique and at 15 GHz by SPDR with the help of a Vector network analyzer (Agilent Technologies, E5071C, ENA Series) [21]. The thermal ageing of the BR–BST composites were performed at 75 °C for 1–11 days in an air oven and the microwave dielectric properties were measured using SPDR. The moisture absorption characteristics of the composites were measured by following the ASTM D 570-98 procedure [22]. The samples with dimensions 50 mm × 50 mm × 2 mm were weighed accurately and immersed in distilled water for 24 h. The samples were then taken out and again weighed after removing excess water from the surface. The volume% of water absorption was then calculated using the relation

$$\text{Volume\% water absorption} = \frac{(W_f - W_i)/\rho_w}{(W_f - W_i)/\rho_w + W_i/\rho_c} \times 100 \qquad (1)$$

where W_i and W_f are the initial and final weights of the sample and ρ_w and ρ_c are the densities of distilled water and sample respectively.

The microwave dielectric properties of the BR–BST composites were investigated before and after immersing the samples in water. The samples were then dried at 60 °C for 2 h and again dielectric properties were measured at 5 GHz. The samples are bent manually by an angle of 180°. The bending cycle was repeated for 125 times and the microwave dielectric properties were investigated after each 25 cycles. The linear coefficient of thermal expansion of each composite was measured using a dilatometer (Netzsch Model, DIL 402 PC)

Table 1
Formulation of the composites used.

Ingredients[a]	**BR–BST-0**	**BR–BST-1**	**BR–BST-2**	**BR–BST-3**	**BR–BST-4**	**BR–BST-5**	**BR–BST-6**	**BR–BST-7**
Butyl rubber	100	100	100	100	100	100	100	100
Zinc oxide	5	5	5	5	5	5	5	5
Stearic acid	3	3	3	3	3	3	3	3
Tetra methyl thiuram disulfide	1	1	1	1	1	1	1	1
Sulfur	0.5	0.5	0.5	0.5	0.5	0.5	0.5	0.5
BST[b]	0	10 (0.016)	25 (0.038)	50 (0.074)	100 (0.14)	200 (0.24)	300 (0.32)	400 (0.39)

[a] Parts per hundred.

[b] The corresponding BST volume fraction is given in parenthesis.

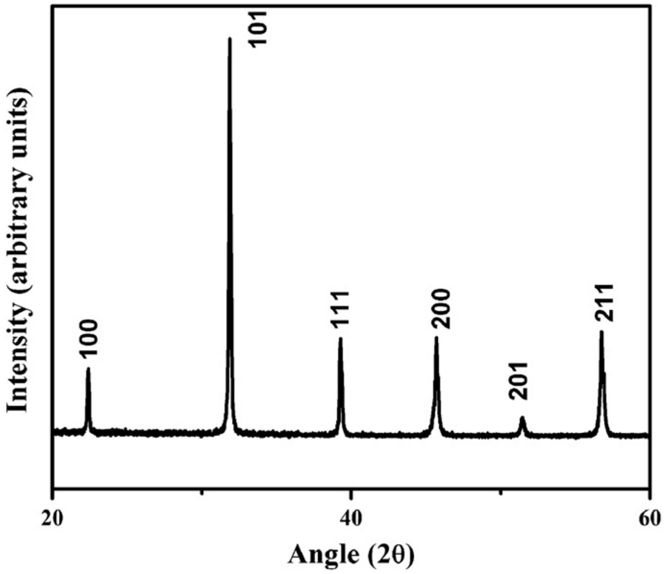

Fig. 1. XRD pattern of $Ba_{0.7}Sr_{0.3}TiO_3$.

in the temperature range from 30 °C to 100 °C at a heating rate of 2 °C/min.

3. Results and discussion

3.1. XRD

Fig. 1 illustrates the XRD pattern of $Ba_{0.7}Sr_{0.3}TiO_3$ ceramic powder sintered at 1300 °C for 4 h. The powder diffraction patterns of $Ba_{0.7}Sr_{0.3}TiO_3$ were indexed based on the JCPDS File no. 44-0093. The single phase of the tetragonal system was confirmed from the XRD.

3.2. Microstructure

Fig. 2(a) shows the SEM image of BST powder which is irregularly shaped. The surface morphologies of BR–BST-1 and BR–BST-7 composites have been shown in Fig. 2(b) and (c), respectively. Both the composites show a uniform dispersion of filler particles in the matrix but at higher filler content some pores and agglomeration of the particles are observed. Dispersion of the particles in the rubber matrix for maximum filler loading is also depicted in Fig. 2(d) which is the fractured surface of the BR–BST-7 composite.

3.3. Mechanical properties

The mechanical flexibility is a prime requirement for a material to be used for flexible applications. Fig. 3 shows the stress strain characteristics of butyl rubber–BST composites. The mechanical properties of the elastomers are generally improved by the addition of ceramic particles. The stress–strain curves of particulate filler-rubber systems depend on the extent of polymer filler interaction and the degree of wetting of filler particles by the polymer matrix [23]. The stiffness of the composite increases with filler content.

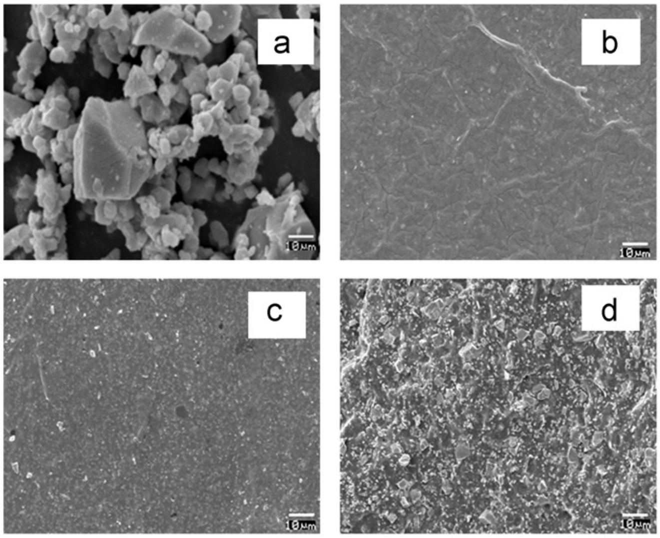

Fig. 2. SEM image of (a) BST powder (b) BR–BST-1 (c) BR–BST-7 and (d) fractured surface of BR–BST-7.

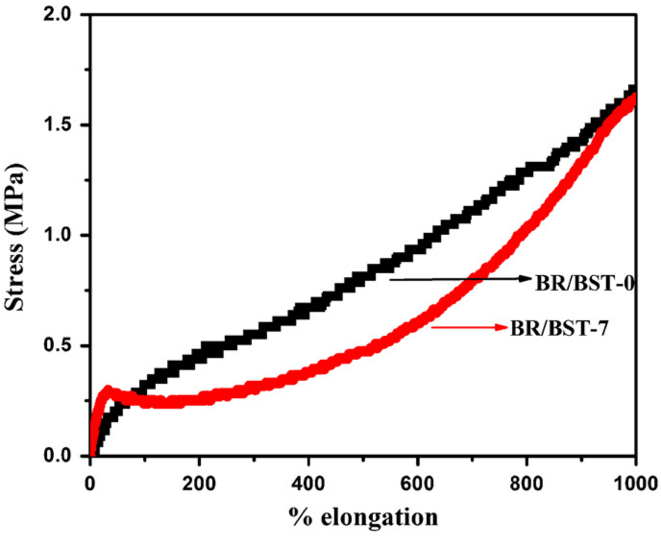

Fig. 3. Stress–strain curves of BR–BST composites.

The BR–BST-7 composite is not broken even upto an elongation of 1000%. This shows the good flexibility and stretchability of the composite.

3.4. Dielectric properties

Fig. 4(a) shows the variation of relative permittivity of BR–BST composites with filler loading at 1 MHz, 5 GHz (measured by both cavity perturbation and SPDR methods) and 15 GHz. From the figure it is clear that ε_r increases with the filler content at all the frequencies. This increasing trend of ε_r is expected since the relative permittivity of BST is very much higher than that of the rubber matrix. The effective dielectric properties are mainly influenced by the interface regions [24]. The butyl rubber–BST composites have interface regions between the elastomer and the ceramic. As the

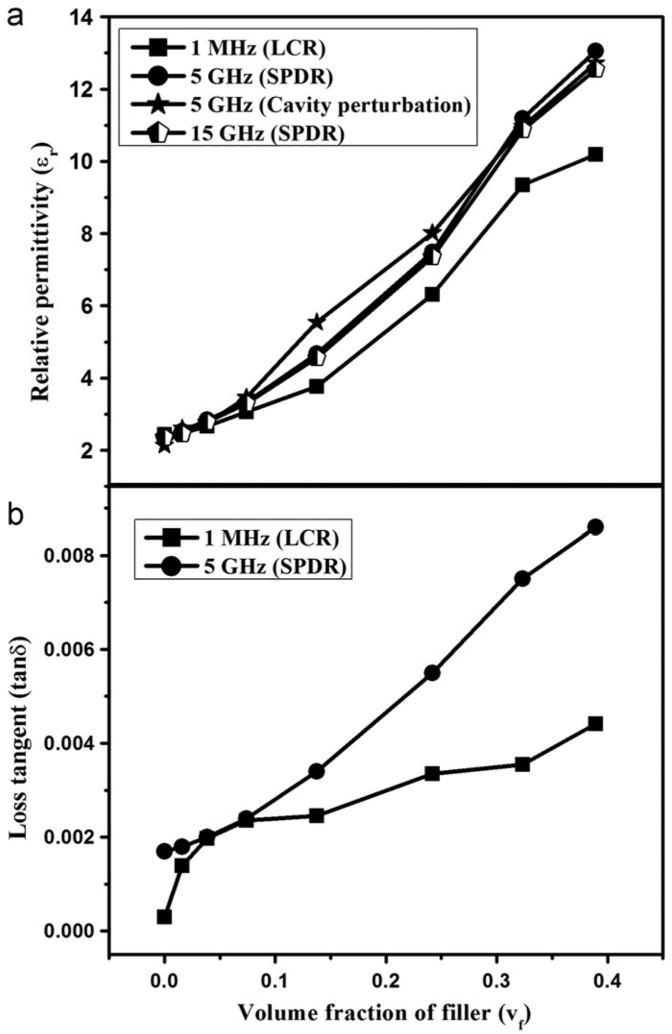

Fig. 4. Variation of (a) relative permittivity and (b) loss tangent with filler loading of BR–BST composites.

filler content increases the interfacial area increases and influence the dielectric properties significantly. At a low volume fraction of ceramic, the filler forms a dispersed phase in the matrix. The main contribution of relative permittivity comes from the continuous matrix and hence the low relative permittivity. As the filler content increases the connectivity between ceramic particles increases leading to increase in dipole dipole interaction which can also contribute to the increase of relative permittivity but to a smaller extent [25]. Also it is worth to note that the ε_r of the composites at microwave frequencies is found to be slightly larger than that obtained at 1 MHz. This may be attributed to some resonance phenomena taking place in the composite. In epoxy–$SrTiO_3$ composites, it has been reported that a resonance absorption occurs in the frequency range from about 5 GHz to 10 GHz during which both the real and imaginary parts of the complex permittivity reaches a maximum at a particular frequency [26]. Similar behavior was observed in our previous reports on butyl rubber composites [13,14]. Further studies are needed to understand the reason for a lower ε_r in the radio frequency range in butyl rubber composites.

Fig. 4(b) shows the variation of loss tangent of BR–BST composites with ceramic content. The loss tangent shows an increasing trend with filler volume fraction as the BST has high loss tangent than the rubber matrix. The dielectric loss of polymers mainly depends on the dipolar impurities, end groups, chain fold, branch point etc. [27]. The dielectric loss will be lower if the concentration of these groups is lower. The dielectric loss of a polymer–ceramic composite depends on the factors such as porosity, moisture content and interface between two components in the composite. The interfacial area increases with filler loading. Hence the accumulation of space charges at the interface of heterogeneous system increases which in turn leads to the increase in dielectric loss at low frequencies [14]. The interfacial polarization is inactive at high frequencies. The large dielectric loss may be due to the large loss from the dipole relaxation of water at microwave frequency [28]. The composite absorbs moisture as the filler content increases and are discussed in Section 3.8. The butyl rubber–BST composites with maximum filler loading of $0.39v_f$ have a loss tangent of 0.004 and 0.009 at 1 MHz and 5 GHz respectively.

3.5. Temperature dependence of relative permittivity at 1 MHz

Fig. 5 shows the temperature dependence of relative permittivity for different ceramic loadings. The relative permittivity of polymer composites should be stable within the operational temperature range of electronic devices for practical applications. From the figure it is clear that all the BR–BST composites are almost stable within the measured temperature range. As the temperature increases the relative permittivity decreases for all the composites. This may be due to the difference in CTE of rubber and filler which would disturb the aggregation of polar fillers and thus reduces the relative permittivity [29,30].

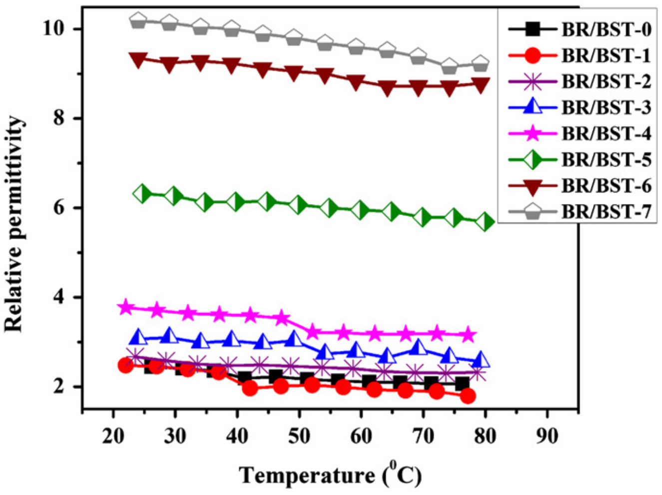

Fig. 5. Temperature dependence of relative permittivity at 1 MHz.

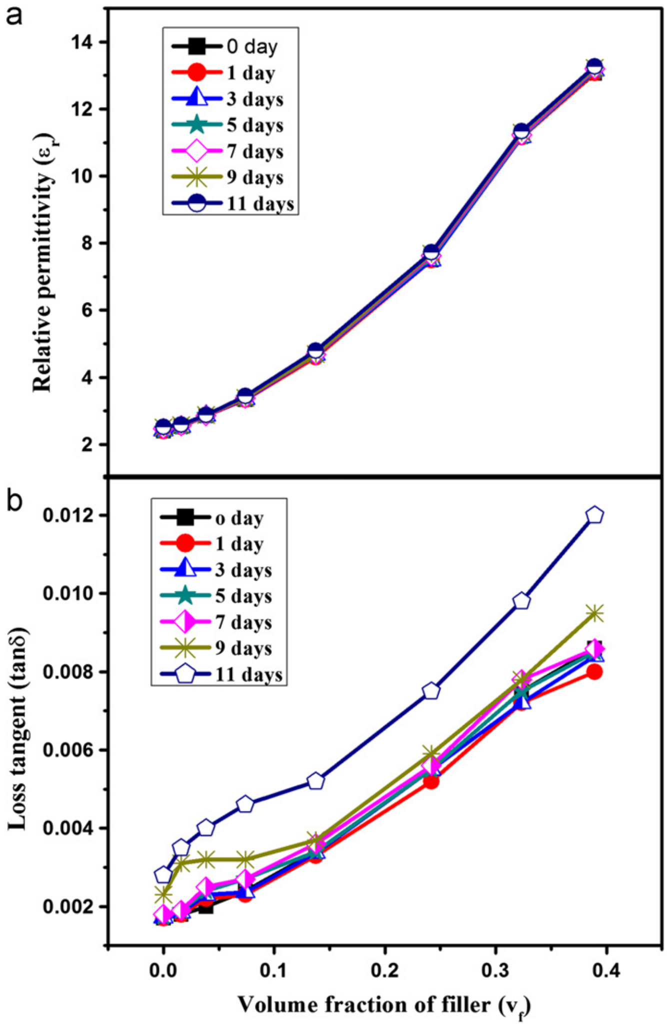

Fig. 6. Variation of (a) relative permittivity and (b) loss tangent with ageing at 75°C for different durations for all compositions at 5 GHz.

3.6. Thermal ageing

Fig. 6(a) and (b) shows the variation of relative permittivity and loss tangent with thermal ageing at 75 °C for different durations of BR–BST composites respectively. The ε_r is almost independent of thermal ageing. But the loss factor increases with ageing time. This may be due to some chemical reactions occurring during ageing [31]. A similar behavior is observed by Overton et al. for teflon films at 50 Hz [32].

3.7. Theoretical modeling

The precise prediction of relative permittivity of the composite using the relative permittivity of the components and the volume fraction of the filler is very important for the design of composites for electronic applications. The composites are considered as heterogeneous systems and their dielectric properties are influenced not only by the relative permittivities of the components but also by other factors such as the morphology, dispersion and the interaction between the two phases. The following models are used to calculate the effective relative permittivity of BR–BST composites: [11]

Jayasundere–Smith equation:

$$\varepsilon_{\mathrm{eff}} = \frac{\varepsilon_m(1-v_f)+\varepsilon_f v_f\left[3\varepsilon_m/(\varepsilon_i+2\varepsilon_m)\right][1+(3v_f(\varepsilon_f-\varepsilon_m)/\varepsilon_i+2\varepsilon_m)]}{1-v_f+v_f[3\varepsilon_m/(\varepsilon_f+2\varepsilon_m)][1+\left(3v_f(\varepsilon_f-\varepsilon_m)/\varepsilon_f+2\varepsilon_m\right)]} \qquad (2)$$

Lichtenecker equation:

$$\ln\varepsilon_{\mathrm{eff}} = (1-v_f)\ln\varepsilon_m + v_f\ln\varepsilon_f \qquad (3)$$

Maxwell–Garnet equation:

$$\varepsilon_{\mathrm{eff}} = \varepsilon_m\frac{2\varepsilon_m+\varepsilon_f+2v_f(\varepsilon_f-\varepsilon_m)}{2\varepsilon_m+\varepsilon_f-v_f(\varepsilon_f-\varepsilon_m)} \qquad (4)$$

Effective Medium Theory:

$$\varepsilon_{\mathrm{eff}} = \varepsilon_m\left[1+\frac{v_f(\varepsilon_f-\varepsilon_m)}{\varepsilon_m+n(1-v_f)(\varepsilon_f-\varepsilon_m)}\right] \qquad (5)$$

where $\varepsilon_{\mathrm{eff}}$, ε_f, ε_m are the relative permittivity of the composites, filler and matrix respectively and v_f is the volume fraction of the filler.

Fig. 7 shows comparison of the experimental values of ε_r with Lichnetcker, Maxwell Garnet equation, Jayasundere Smith equation and the Effective Medium Theory (EMT) model. From the figure it is clear that Lichnetcker and Maxwell Garnet equations hold good for low filler contents [33,34]. This may be due to the imperfect dispersion of ceramic particles at higher filler loading. The Jayasundere Smith equation is also not matching with the experimental values. In the Jayasundere Smith model all the ceramic particles are considered to be spherical in shape. The BST particles are irregularly shaped in the present investigation which is evident from the SEM image in Fig. 2(a). Hence this model shows deviation from experimental values [35]. The experimental relative permittivity is in good agreement with the EMT model [36]. According to this model the composite is considered as effective medium

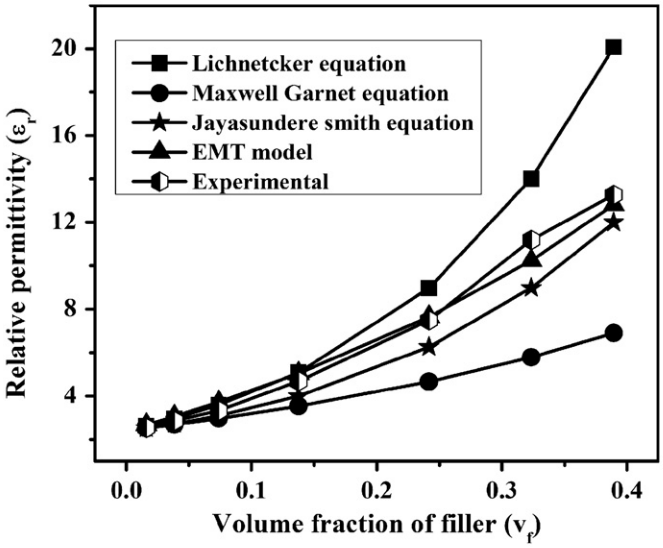

Fig. 7. Comparison between experimental and theoretical relative permittivity with BST loading at 5 GHz.

whose effective relative permittivity is obtained by averaging over the relative permittivity of the two constituents. EMT model is a self consistent model which assumes a random unit cell (RUC) consisting of each filler surrounded by a concentric matrix layer. When a RUC is embedded in an effective medium it cannot be detected in an electromagnetic experiment. This model incorporates a shape factor '*n*', which is subjected to the shape of ceramic particles. The value of *n* for BR–BST composite is found to be 0.17 which is in agreement with our previous report [14]. Since the EMT model includes a shape factor there is no restriction with the shape of the ceramic particles. Hence it is very well matching with experimental values.

3.8. Moisture absorption

Fig. 8 shows the moisture content of BR–BST composites as a function of ceramic loading. The polymer–ceramic composites are very sensitive to humidity. Since water is a polar molecule with high ε_r and tan δ it will seriously affect the dielectric properties of the composites. From the figure it is clear that the volume% of moisture increases with filler volume fraction. The volume of polymer–ceramic interface increases with filler loading which in turn promotes moisture absorption [37,38]. The increasing trend may be due to the presence of pores which is evident from the SEM image in Fig. 2(c).

Fig. 9(a) and (b) shows the variation of microwave dielectric properties of the composites with filler loading before and after immersing the samples in water for 24 h, respectively at 5 GHz. Then the samples are taken out and dried at 60 °C for 2 h. Again microwave dielectric properties are studied as a function of ceramic content. The relative permittivities of the composites before and after water immersion are almost same. But after drying it slightly decreases with the ceramic content. The loss tangent of BR–BST composites is slightly higher after water absorption. This may be due to the high relative permittivity and loss tangent of water. Similar behavior was observed by Hakim et al. in natural rubber-intermediate super abrasion furnace (ISAF) composites [39].The loss tangent decreases for composites after drying. This may be due to the evaporation of water during drying.

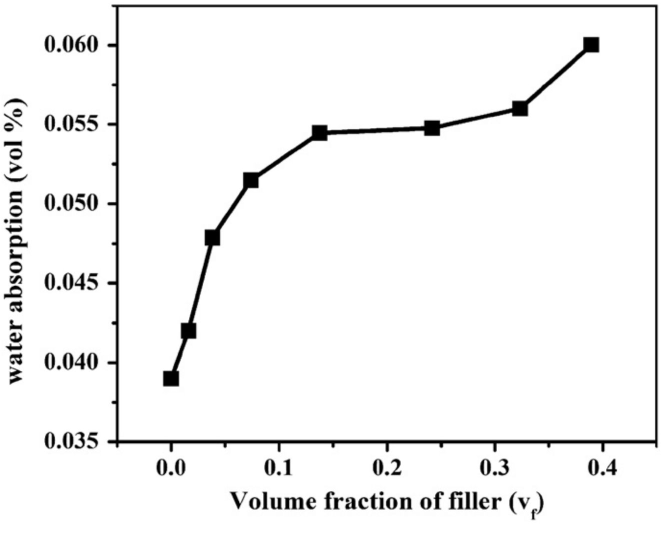

Fig. 8. Variation of moisture absorption with filler content of BR–BST composites.

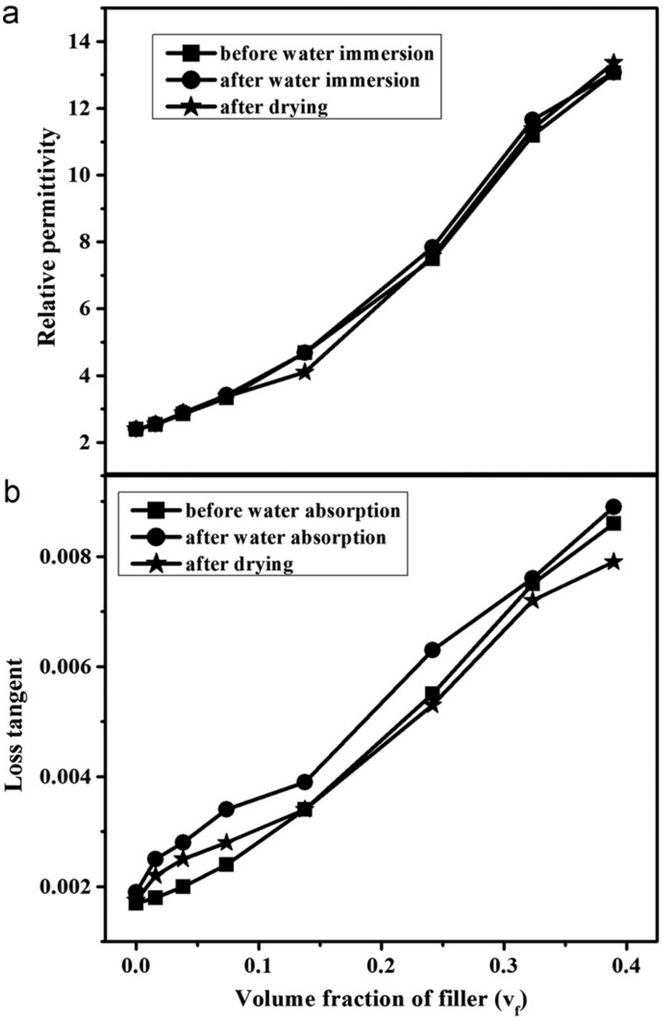

Fig. 9. Variation of (a) relative permittivity and (b) loss tangent with filler content before and after water immersion and after dried at 60 °C for 2 h.

3.9. Bending

Fig. 10 shows the variation of microwave dielectric properties of BR–BST composites after repeated bending of samples by an angle of 180°. From the figure it is clear that the relative permittivity of the composites are almost independent of bending upto a volume fraction of 0.32 and after that it slightly decreases after 25 cycles of bending. The loss tangent of the butyl rubber–BST composites is also almost constant throughout the repeated bending upto a filler loading of $0.24v_f$ and the loss tangent shows a slight variation after a volume fraction of 0.24. The deviation at higher filler loading may be due to the particle agglomeration at the higher filler content [40].Similar result is observed in our previous report [14].

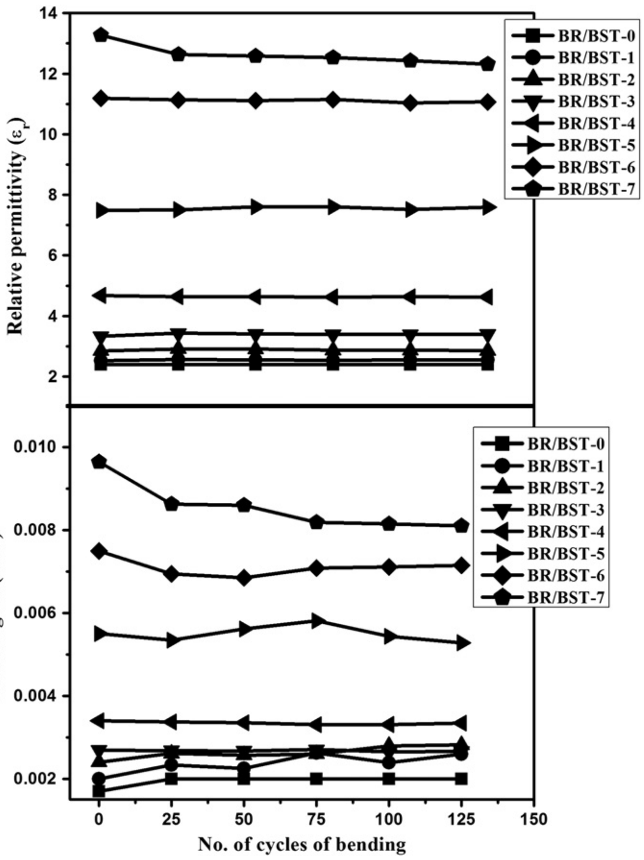

Fig. 10. Variation of microwave dielectric properties of BR–BST composites with bending.

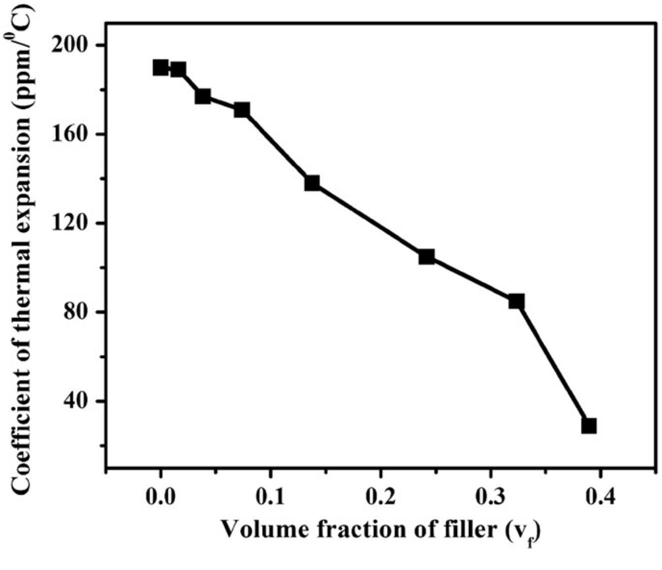

Fig. 11. Variation of CTE of butyl rubber–BST composites with BST loading.

3.10. Coefficient of thermal expansion

Fig. 11 shows the variation of coefficient of thermal expansion (CTE) of BR–BST composites with filler content. The CTE of pure rubber matrix is 190 ppm/°C. As the filler volume fraction increases, the CTE decreases. When a composite is heated, the polymer matrix will expand more than that of ceramic fillers. The expansion of matrix will be reduced if the interfaces are capable of transmitting stress. The polymer chains get arrested in the presence of ceramic and will be unable to expand with temperature. Hence the CTE of a composite is reduced with increase in filler content and composite with strong interface exhibit an additional reduction of CTE [41,42].

4. Conclusion

BR–BST composites were prepared by sigma mixing followed by hot pressing. The microstructure of the composites shows a homogenous dispersion of ceramic particles in the rubber matrix. The dielectric properties of the composites were improved with filler loading both at radio and microwave frequencies. The BR–BST-7 composite attained a relative permittivity of 13.1 and loss tangent of 0.009 at 5 GHz measured by SPDR. All the butyl rubber–BST composites are almost thermally stable within the measured temperature range. The ε_r and tan δ of the BR–BST composites were investigated with ageing time and with bending at 5 GHz. The EMT model is in good agreement with experimental $\varepsilon_{r.}$ The moisture content of the composites increases with filler loading. The CTE of butyl rubber composites are found to be decreased with filler content. All the measured properties indicate that the butyl rubber–BST composite is suitable for flexible dielectric wave guide applications.

Acknowledgment

The authors are grateful to the Council of Scientific and Industrial Research (CSIR), India for the award of Senior Research Fellowship. The authors are thankful to Dr. P. Prabhakar Rao and Mr. M.R. Chandran for SEM, and Mr. Brahmakumar for tensile measurements.

References

[1] D.H. Kim, J.A. Rogers, Stretchable electronics: materials strategies and devices, Advanced Materials 20 (2008) 4887–4892.

[2] A. Ostmann, T. Loher, M. Seckel, L. Bottcher, H. Reichl, Manufacturing concepts for stretchable electronic systems, IEEE (2008) 24–27.

[3] T. Sekitani, Y. Noguchi, K. Hata, T. Fukushima, T. Aida, T. Someya, A rubber like stretchable active matrix using elastic conductors, Science Magazine 321 (2008) 1468–1472.

[4] M. Gonzalez, F. Axis, M.V. Bulcke, D. Brosteaux, B. Vandevelde, J. Vanfleteren, Design of metal interconnects for stretchable electronic circuits, Microelectronics Reliability 48 (2008) 825–832.

[5] J.A. Rogers, Y.G. Huang, A curvy, stretchy future for electronics, Proceedings of National Academy of Sciences 106 (2009) 10875–10876.

[6] J. Obrzut, P.F. Goldsmith, Flexible circular waveguides at millimeter wavelengths from metallized teflon tubing, IEEE Transactions on Microwave Theory and Techniques 38 (1990) 324–327.

[7] W.M. Bruno, W.B. Bridges, Flexible dielectric waveguides with powder cores, IEEE Transactions on Microwave Theory and Techniques 36 (1988) 882–890.

[8] T. Joseph, S. Uma, J. Philip, M.T. Sebastian, Dielectric, thermal and mechanical properties of $Sr_2ZnSi_2O_7$ based polymer ceramic composites, Journal of Materials Science: Materials in Electronics 23 (2012) 1243–1254.

[9] S. Thomas, V.N. Deepu, P. Mohanan, M.T. Sebastian, Effect of filler content on the dielectric properties of PTFE/$ZnAl_2O_4$–TiO_2 composites, Journal of the American Ceramic Society 91 (2008) 1971–1975.

[10] G. Subodh, M. Joseph, P. Mohanan, M.T. Sebastian, Low dielectric loss polytetrafluoroethylene/TeO_2 polymer ceramic composites, Journal of the American Ceramic Society 90 (2007) 3507–3511.

[11] M.T. Sebastian, H. Jantunen, Polymer–ceramic composites of 0–3 connectivity for circuits in electronics: a review, International Journal of Applied Ceramic Technology 7 (2010) 415–434.

[12] F. Xiang, H. Wang, X. Yao, Dielectric properties of $SrTiO_3$/POE flexible composites for microwave applications, Journal of the European Ceramic Society 27 (2007) 3093–3097.

[13] C. Janardhanan, D. Thomas, G. Subodh, S. Harshan, J. Philip, M.T. Sebastian, Microwave dielectric properties of flexible butyl rubber–strontium cerium titanate composites, Journal of Applied Polymer Science 124 (2012) 3426–3433.

[14] D. Thomas, C. Janardhanan, M.T. Sebastian, Mechanically flexible butyl rubber–$SrTiO_3$ composite dielectrics for microwave applications, International Journal of Applied Ceramic Technology 8 (2011) 1099–1107.

[15] I.K. Hakim, A.M. Bishai, A.L. Saad, Dielectric properties of butyl rubber mixtures at 10^6–10^{10} Hz, Journal of Applied Polymer Science 35 (1988) 1123–1125.

[16] B.R. Priya Rani, M.T. Sebastian, The effect of glass addition on the dielectric properties of barium strontium titanate, Journal of Materials Science: Materials in Electronics 19 (2008) 39–44.

[17] T. Hu, J. Juuti, H. Jantunen, T. Vilkman, Dielectric properties of BST/polymer composite, Journal of the European Ceramic Society 27 (2007) 3997–4001.

[18] H. Wang, F. Xiang, K. Li, Ceramic polymer $Ba_{0.6}Sr_{0.4}TiO_3$/ poly (methyl methacrylate) composites with different type composite structures for electronic technology, International Journal of Applied Ceramic Technology 7 (2010) 435–443.

[19] J.W. Liou, B.S. Chiou, Dielectric tunability of barium strontium titanate/silicone-rubber composite, Journal of Physics: Condensed Matter 10 (1998) 2773–2786.

[20] H. Barron, Modern Synthetic Rubbers, Chapman & Hall, London, 1949.

[21] M.T. Sebastian, in: Dielectric Materials for Wireless Communications, 1st ed, Elsevier, Oxford, UK, 2008.

[22] P.S. Anjana, V. Deepu, S. Uma, P. Mohanan, J. Philip, M.T. Sebastian, Dielectric, thermal, and mechanical properties of CeO_2-filled HDPE composites for microwave substrate applications, Journal of Polymer Science: Polymer Physics 48 (2010) 998–1008.

[23] S.A. AL-Gahtani, Mechanical properties of acrylonitrile butadiene/ ethylene propylene diene monomer: effects of blend ratio and filler addition, Journal of American Science 7 (2011) 804–809.

[24] M.G. Todd, F.G. Shi, Validation of a novel dielectric constant simulation model and the determination of its physical parameters, Microelectronics Journal 33 (2002) 627–632.

[25] D.H. Kuo, C.C. Chang, T.Y. Su, W.K. Wang, B.Y. Lin, Dielectric properties of three ceramic/epoxy composites, Materials Chemistry and Physics 85 (2004) 201–206.

[26] H.D. Choi, H.W. Shim, K.Y. Cho, H.J. Lee, C.S. Park, H.G. Yoon, Electromagnetic and electromagnetic wave-absorbing properties of the $SrTiO_3$–epoxy composite, Journal of Applied Polymer Science 72 (1999) 75–83.

[27] S. George, V.N. Deepu, P. Mohanan, M.T. Sebastian, Influence of $Ca[(Li_{1/3}Nb_{2/3})_{0.8}Ti_{0.2}]O_{3-d}$ filler on the microwave dielectric properties of polyethylene and polystyrene for microelectronic applications, Polymer Engineering and Science 50 (2010) 570–576.

[28] F. Xiang, H. Wang, X. Yao, Preparation and dielectric properties of bismuth-based dielectric/PTFE microwave composites, Journal of the European Ceramic Society 26 (2006) 1999–2002.

[29] S.H. Xie, B.K. Zhu, X.Z. Wei, Z.K. Xu, Y.Y. Xu, Polyimide/$BaTiO_3$ composites with controllable dielectric properties, Composites: Part A 36 (2005) 1152–1157.

[30] M.A. Berger, R.L. Mc Cullough, Characterization and analysis of the electrical properties of a metal-filled polymer, Composites Science and Technology 22 (1985) 81–106.

[31] Y.Y. Sun, S. Luo, C.P. Wong, Electrical and mechanical properties of carbon black filled ethylene propylene rubber during thermal oxidation ageing, in: Electronic Components and Technology Conference, 2003, pp. 1644–1647.

[32] E. Overton, A.N. Hammoud, E.D. Baumann, I.T. Myers, Thermal aging effects on the electrical properties of film and ceramic capacitors, Electrical Electronics Insulation Conference and Electrical manufacturing and Coil Winding Conference, 1993, 201–205.

[33] A.V. Goncharenko, V.Z. Lozovski, E.F. Venger, Lichtenecker's equation: applicability and limitations, Optics Communication 174 (2000) 19–32.

[34] F. Claro, R. Rojas, Correlation and multipolar effects in the dielectric response of particulate matter: an interactive mean field theory, Physical Review B 43 (1991) 6369–6375.

[35] N. Jayasundere, B.V. Smith, Dielectric-constant for binary piezoelectric 0–3 composites, Journal of Applied Physics 73 (1993) 2462–2466.

[36] Y. Rao, J. Qu, T. Marinis, C.P. Wong, A precise numerical prediction of effective dielectric constant for polymer–ceramic composite based on effective-medium theory, IEEE Transactions on Components and Packaging Technologies 23 (2000) 680–683.

[37] P. Gonon, T. Pham Hong, O. Lesaint, S. Bourdelais, H. Debruyne, Influence of high levels of water absorption on the resistivity and dielectric permittivity of epoxy composites, Polymer Testing 24 (2005) 799–804.

[38] H. Zhao, R.K.Y. Li, Effect of water absorption on the mechanical and dielectric properties of nano-alumina filled epoxy nano composites, Composites: Part A 39 (2008) 602–611.

[39] I.K. Hakim, A.W. Aziz, K.N.A. Nour, Environmental effects and relaxation in natural rubber, Journal of Applied Polymer Science 33 (1987) 2439–2447.

[40] A.A.M. Ward, B. Stoll, W.V. Soden, S. Herminghaus, A.A. Mansour, Effect of cyclic deformations on the dynamic-mechanical properties of silica-filled butyl rubber, Macromolecular Materials and Engineering 278 (2003) 971–979.

[41] L. Holliday, Robinson, review: the thermal expansion of composites based on polymers, Journal of Materials Science 8 (1973) 301–311.

[42] R.K. Goyal, A.N. Tiwari, U.P. Mulik, Y.S. Negi, Novel high performance Al_2O_3/poly(ether ether ketone) nanocomposites for electronics applications, Composites Science and Technology 67 (2007) 1802–1812.